ISSN 1330-3651 (Print), ISSN 1848-6339 (Online)
https://doi.org/10.17559/TV-20230628000771
Original scientific paper

Experimental Study of the Product Layer Effect in the Process of Mortar under Corrosion in Sulfuric Acid

Weihang ZHANG, Zhigang SONG*

Abstract: A product layer will grow on the surface of cement mortar when the sulfuric acid attacks the former, which created the blocking effect to the corrosion process and damps the reaction rate. To investigate the surface coating effect, long time immersion tests in sulfuric acid were conducted on two batches of cement mortar specimens. For comparison, product layer removal and acid replacement were conducted regularly on one batch, while the other batch remained unchanged during the whole process. The apparent diffusion coefficients of mortar at different immersion time were calculated by the model of dissolution reaction and experiment datum. The changing of the apparent diffusion coefficients in different batch and at different immersion time was obtained. Scanning electron microscopy and X-ray diffraction were used for analysis of the morphology and phase composition of the product layer. The results indicate that the surface coating effect exists no matter the immersion acid was replaced or not. However, by replacing the immersion acid and removing the product layer, the influence of the blocking effect is reduced and the corrosion rate is increased. The apparent diffusion coefficients observed in both batches will decrease according to the power law of immersion time.

Keywords: cement mortar; corrosion; microstructure; sulfuric acid; surface coating effect

1 INTRODUCTION

In the last two decades, there were lots of field observations on the degradation of concrete or mortar by sulfuric acid from variety service environments such as acid rain, industrial process and sewage system [1-4]. It is generally believed that the reaction between sulfuric acid and calcium hydroxide in cement stone produces calcium sulfate, which is poorly water-soluble [5-9]. When it reaches a certain concentration, it precipitates as a solid on the surface of the reactant. During hydrometallurgy the solid product layer covering the reactant surface is called the product layer, and the effect of the product layer slowing down the chemical reaction is called the surface coating effect [10-12]. Study by Israel et al. [13] showed that when concrete is attacked by sulfuric acid, an adherent layer is produced on the surface of the corrosion layer, while nitric acid and hydrochloric acid do not produce such adherent layer. Monteny et al. [14] propose that a barrier layer is formed during the corrosion of concrete by sulfuric acid, which blocks the reaction between the two. Gutberlet et al. [15] however propose that the main component of sulfate-eroded concrete surfacing layer is calcium sulfate and ettringite, which will lead to concrete cracking due to swelling, thus aggravating the corrosion of concrete by sulfuric acid. From long period of immersion test of concrete in sulfuric acid, Xie et al. [16] observed that the solution rate decreases first before increasing and finally becoming steady, and suggested that the formation of the product layer is the result of the generating-solving competition mechanism. Min et al.[17] by long-term immersion test obtained the reaction rate curve of sulfuric acid attaching concrete and found it has a sudden decline in the late period of reaction, and the curve showed an obvious "trailing" phenomenon, and proposes that such phenomenon is related to coating of concrete surface by the calcium sulfate generated during the corrosion process. Feng et al. [18] analyzed the product layer of concrete corroded by sulfuric acid and found its main component is sulfuric calcium and no trace of ettringite was found.

In order to study the influence of surface coating effect on the corrosion of cement mortar by sulfuric acid and the composition of such product layer, we conducted a long time immersion test on two batches of cement mortar specimens in sulfuric acid. For one batch of specimens, the corrosion product layers were removed and the immersion liquid replaced periodically to eliminate the blocking effect of product layer on the corrosion process. The total amount of sulfuric acid consumed by the two patches of specimens was recorded and the theoretical consumption of acid was also obtained using the corrosion-dissolution process model proposed by Song et al. [19] while assuming the diffusion coefficient as a constant. The theoretical prediction was compared with the actual consumption of acid from experiments. The possibility of calcium sulfate precipitation was also analyzed, and scanning electron microscopy and X-ray diffraction were used for analysis of the morphology and phase composition of the product layer.

2 MATERIALS AND METHODS

2.1 Materials

The cement used in the test is PO 42.5 ordinary Portland cement (C). The sand is selected as special sand for perfusion procedure. The particle size of the sand ranges between 0.25 and 0.65 mm. The SiO_2 content is larger than 96% and mud content (including soluble salts) less than 0.20%; loss on ignition is less than 0.40%. The sulfuric acid is bought from in Shanghai Sulfuric Acid Factory (mass fraction > 98%, density 1.84 g/cm^3, analytical grade).

2.2 Methods

In accordance with GBT 17671-1999 "cement mortar strength test method (ISO method)", 60 specimens of cement mortar (size: 16 cm × 4 cm × 4 cm) were made and divided into 10 groups, with 6 specimens in each group. After the vibration-molding procedure, they were put in a standard curing box (constant temperature of 20 ℃, relative humidity of 95%) for 24 h. The corrosive liquid is

diluted sulfuric acid with pH of 4.0, the experimental setup is shown in Fig. 1, and the procedure is listed in Tab. 1. After demolding, the specimens were again cured for 28 days in saturated sodium hydroxide solution. The interior of the room was allowed to dry naturally for 7 days after the curing. The floating paste attached to the surface of the specimens was removed with a metal brush. A total of 4 surfaces of the specimens (upper, lower and both ends) were sealed with liquid paraffin. After the immersion starts, the pH of the acid solution was monitored using a pHB-1 pH meter (accuracy of 0.01), and the titration was proceeded using 0.125 mol/L of dilute sulfuric acid to maintain the pH value of the immersion acid solution. The cumulative amount of sulfuric acid was obtained by summing up the separate consumption of diluted sulfuric acid $M(t)$ in each test.

In order to test the influence of product layer on the consumption of acid, the 6 ~ 10 groups of specimens were removed from the acid solution. The attached layer was removed using the fine iron brush before they were put back to the immersion liquid again. For comparison, the 1 ~ 5 groups of the specimens did not go through the above procedure.

After 90 days, the mortar specimens were taken out and the different groups were respectively specimen for microscopic analysis. The FEI Quanta 200 FEG scanning electron microscope was used to observe the microstructure of the specimens under high vacuum mode after sulfuric acid corrosion. The phase composition of the corrosion layer of the specimen after etching with sulfuric acid was analyzed by TTR III X-ray diffractometer (Cu Kα, operating voltage 45 kV, operating current 200 mA). The measurement mode was continuous scanning at the scanning rate of 8 °/min.

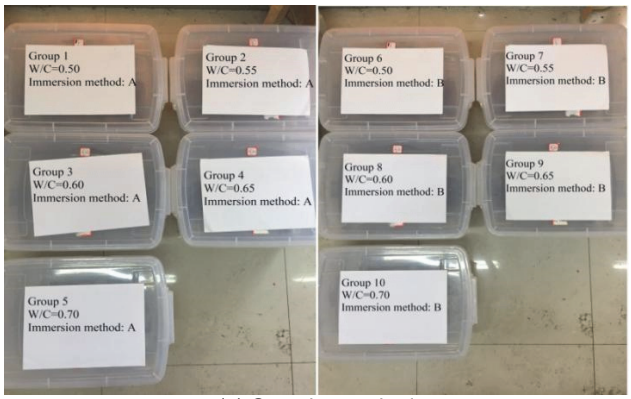

(a) Grouping method

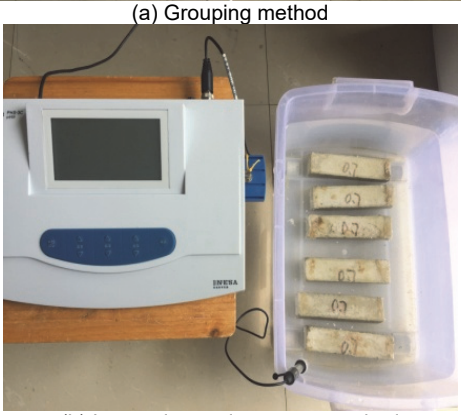

(b) Immersion and measure method

Figure 1 Test arrangement

Table 1 Mixture proportion and pH value of solution

Group	Mix proportion (by mass)			pH	Specimen number of each group	Immersion method
	S	C	W			
1	3	1	0.50	4.0	6	A
2	3	1	0.55	4.0	6	A
3	3	1	0.60	4.0	6	A
4	3	1	0.65	4.0	6	A
5	3	1	0.70	4.0	6	A
6	3	1	0.50	4.0	6	B
7	3	1	0.55	4.0	6	B
8	3	1	0.60	4.0	6	B
9	3	1	0.65	4.0	6	B
10	3	1	0.70	4.0	6	B

Immersion method: A. Immersion, surface cleaning and solution replacement. B. Immersion without cleaning.

3 RESULTS AND DISCUSSION

3.1 Total Acid Consumption

The cumulative consumption of sulfuric acid by each group of specimens was collected at the end of the test and the results were summarized in Fig. 2.

It can be seen from Fig. 2 that the two batches of specimens consumed approximately same amount of acid at around 500 h of immersion. However, the consumption of acid by specimen groups of 1 ~ 5 became significantly larger than sets of 6 ~ 10 after 500 h.

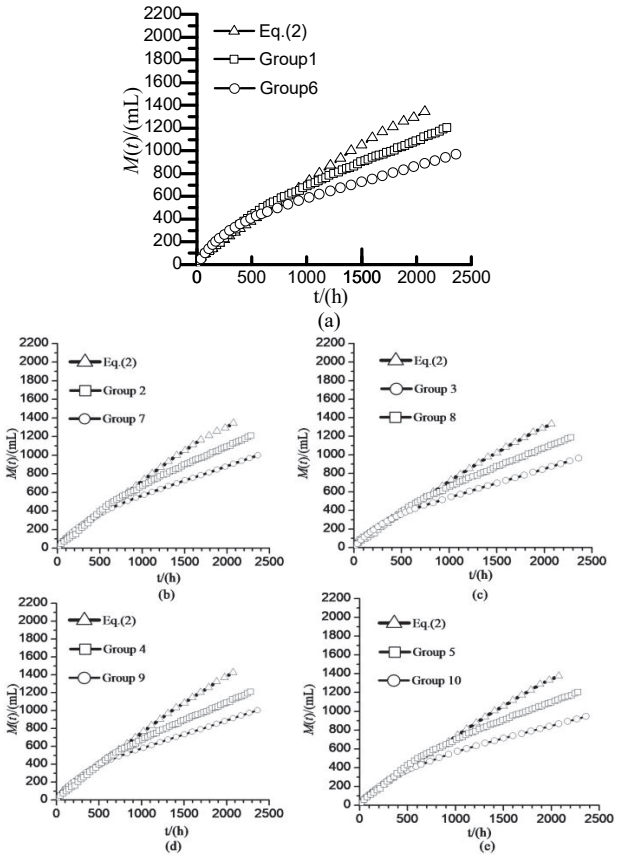

Figure 2 Actual and theoretical acid consumption of the specimen

Before the reaction proceeds to 500 h, the sulfuric attacks the cement mortar at a fast rate. At this time, the influence of the formation of corrosion layer on the corrosion rate is negligible. The corrosion rate mainly depends on the dissolution rate of calcium hydroxide in the mortar [20]. Therefore, neither the removal of the attaching

layer from the surface of the specimen nor the replacement of the soaking liquid have any effect on the corrosion rate, the total amount of acid consumed by the two batches of specimens before 500 h was similar. After 500 h, the corrosion products gradually adhered to the surface of mortar to form an adherent layer. It not only reduces the solution rate of calcium hydroxide in the mortar but also hinders the attacking speed of sulfuric acid on the mortar [21]. Therefore, the performance of 500 h, the group 6 ~ 10 specimen acid consumption was significantly lower than the group 1 ~ 5.

3.2 Dissolution Reaction of Sulfuric Acid Attacking Mortar

The corrosion process of cement mortar by the sulfuric acid is described by Song et al. [22] as:

$$\frac{\partial C_{OH^-}(x,t)}{\partial t} = D_{OH^-}\frac{\partial^2 C_{OH^-}(x,t)}{\partial x^2} - kC_{OH^-}(x,t)C_{H^+}(x,t) \quad (1)$$

where x is the distance from a point in the reaction boundary layer to the unreacted surface in m; t is the reaction time in s; $C_{OH^-}(x, t)$ and $C_{H^+}(x, t)$ are the concentrations of H^+ and OH^- in mol/L; k is the reaction constant in mol^{-1}/s. D_{OH^-} is the diffusion coefficient of OH^- in m^2/s.

$M(t)$, the total consumption of H^+ during the time of t, is expressed as:

$$M(t) = \frac{a}{b}\ln\left[\frac{1+\sqrt{1-\exp(-bt)}}{1-\sqrt{1-\exp(-bt)}}\right] \quad (2)$$

where $a = SC_{OH^-.S}\sqrt{2D_{OH^-}kPC_{H^+.S}}$, $b = 6kPC_{H^+.S}$, $C_{OH^-.s}$ is the concentration of H^+ in over-saturated $Ca(OH)_2$ solution, and $C_{H^+.s}$ is the concentration in solution of H_2SO_4 in mol/L. S is the corrosion surface area in m^2. And D_{OH^-}, the diffusion coefficient is:

$$D_{OH^-.} = \frac{3a^2}{bS^2C^2_{OH^-.S}} \quad (3)$$

Since the diffusion coefficient D_{OH^-} changes constantly during the corrosion process and cannot be measured directly, it can only be obtained by fitting the experimental data. Therefore, the D_{OH^-} value obtained by fitting the test piece data is not an instantaneous diffusion coefficient, but an average diffusion coefficient within the testing time, and is therefore called an apparent diffusion coefficient.

It can be seen from Fig. 2 that the total amount of acid consumed by the two batches of specimens is similar before the reaction reaches 500 h. So we assume that during the initial stage of the reaction the corrosion products have not yet accumulated, the blocking effect of the attached layer on the corrosion is negligible and the diffusion coefficient D_{OH^-} is a constant. And the D_{OH^-} value by fitting the experimental data can be regarded as the actual diffusion coefficient when the surface coating effect is not pronounced.

By fitting the experimental data of the first 500 h with Eq. (2), the value of a, b and the corresponding fitting parameters were obtained and listed in Tab. 2, the fitting curve is shown in Fig. 2. $M(t)$ in Tab. 2 indicates the theoretical value of total amount of acid consumed by the cement mortar.

Table 2 Regression results of experiment results according to Eq. (2)

Group	a / ml/h	$b \times 10^{-4}$ / h^{-1}	Correlation coefficient
1	1.2796	0.0311	0.9914
2	0.8841	0.1236	0.9873
3	0.8585	0.1004	0.9759
4	0.9351	0.1132	0.9908
5	0.9112	0.1236	0.9914

It is seen from Fig. 2 that as the reaction proceeds, the total acid consumption curve of 6 ~ 10 groups of mortar specimens significantly slowed down and gradually stabilized, the cumulative acid consumption curve is located at the bottom and the total consumption of acid is the smallest. The total acid consumption of the groups 1 ~ 5 was higher than that from groups 6 ~ 10, the accumulated acid consumption curve was in the middle, and the total acid consumption was less than the theoretical prediction.

After long-term static immersion test, more and more corrosion products attach to the surface of 6 ~ 10 groups of the cement mortar specimens, forming an interface layer that hinders the reaction and leads to the gradual reduction of sulfuric acid consumption. The consumption of sulfuric acid by the 1 ~ 5 groups of mortar specimens was significantly higher than that of the 6 ~ 10 groups of specimens after regular removal of the product layer and the replacement of immersion. This is because after the attaching layer is removed from the specimen fresh mortar surface is exposed to the replaced acid solution, and the surface coating effect is reduced. However, the acid consumption of 1 ~ 5 groups of specimens was lower than the theoretical prediction, while the latter does not consider the surface coating effect. This may be caused by two factors: a) The corrosion reaction continues while the immersion acid is being replaced, so the reaction products continue to attach to the surface of the specimens, hindering the corrosion of mortar by sulfuric acid; b) There is no guarantee that a thin brush can completely remove the attached layers from the mortar.

3.3 The Time-Dependent Conversion Factor $R_t(t)$

After collecting the testing result, we obtained the change of the apparent diffusion coefficient with time by analyzing the cumulative acid consumption at different immersion time. From Eq. (2) and Eq. (3), we see that the variation of D_{OH^-} with time will only cause a change in a. Therefore, the time-dependent conversion factor $R_t(t)$ can be used to describe the change of the apparent diffusion coefficient as:

$$R(t) = \frac{D_{OH^-}(t)}{D_{OH^-}(t_0)} = \frac{a^2(t)}{a^2(t_0)} \quad (4)$$

where $a(t)$, $D_{OH^-}(t)$, $a(t_0)$, $D_{OH^-}(t_0)$ are the corresponding values of a and D_{OH^-} at the immersion time of t and t_0 respectively.

In order to grasp the changing rule of $R(t)$ with time, Eq. (5) was used to calculate $R(t)$ at different time based on the experimental value of $M(t)$ and the results were shown in Fig. 3. The regression results show that $R(t)$ from all specimen groups is Power function of the immersion time t.

$$R(t) = A(t - t_0)^B \tag{5}$$

where t_0 = 500 h is the experimental reference time, A and B are the regression constants, as shown in Tab. 3.

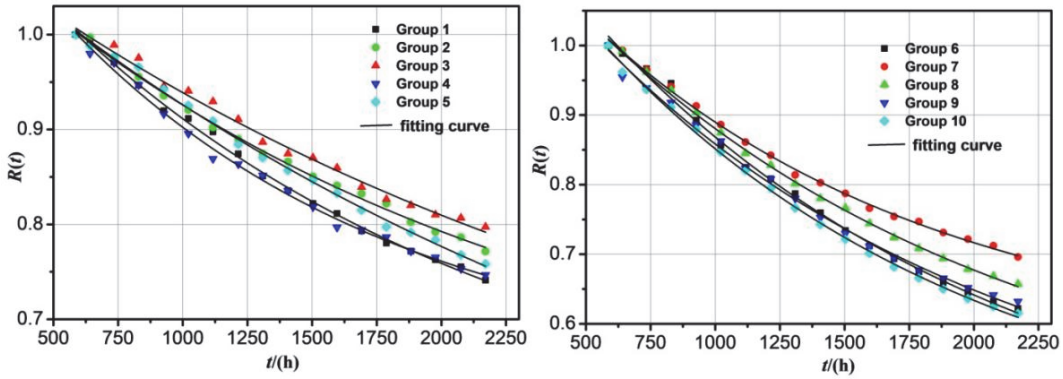

Figure 3 Converted coefficients of the apparent diffusion coefficients

Table 3 Fitting results

Group	1	2	3	4	5	6	7	8	9	10
A	2.21	2.01	2.02	2.04	2.10	1.62	1.52	1.54	1.59	1.58
B	−0.16	−0.13	−0.14	−0.15	−0.15	−0.10	−0.08	−0.09	−0.09	−0.09
R	0.963	0.972	0.951	0.965	0.958	0.974	0.967	0.961	0.965	0.957

As can be seen from Tab. 3, if the product layer is removed and the immersion liquid replaced (groups 1 ~ 5), A varies from 2.01 to 2.21 with the water-cement ratio in the mortar, while B varies between 0.13 ~ −0.16; when the product layer is not removed and the immersion liquid not replaced (groups 6 ~ 10), A varies between 1.52 ~ 1.62 with the water-cement ratio, and B varies between –0.08 ~ –0.10.

3.4 Analysis on the Precipitation of Calcium Sulfate

Previous studies indicate that the following reaction happens during the corrosion of cement mortar by sulfuric acid [23-26]:

$$Ca(OH)_2 + H_2SO_4 \rightarrow CaSO_4 \cdot 2H_2O \tag{6}$$

$$CaO.SiO_2.2H_2O + H_2SO_4 \rightarrow CaSO_4 + H_4SiO_4 + H_2O \tag{7}$$

$$3CaO.Al_2O_3.6H_2O + 3H_2SO_4 \rightarrow 3CaSO_4 + 2\,Al(OH)_3 + 6\,H_2O \tag{8}$$

$$2Al(OH)_3 + 3H_2SO_4 \rightarrow Al_2(SO_4)_3 + 6H_2O \tag{9}$$

The products from the above reactions include $CaSO_4 \cdot 2H_2O$ (slightly soluble), H_4SiO_4 (non-soluble) and $Al_2(SO_4)_3$ (soluble), the unstable H_4SiO_4 will decompose into SiO_2 and H_2O. Therefore, the remainning products which are capable of attaching to the mortar surface are $CaSO_4 \cdot 2H_2O$ and SiO_2. since $CaSO_4 \cdot 2H_2O$ is poorly soluble; whether it can be precipitated needs to be judged by its solubility in dilute sulfuric acid solution.

At 20 °C, the solubility of $CaSO_4 \cdot 2H_2O$ in the solution with pH 4 (0.05 mmol/L sulfuric acid) is 0.0152 mol/L [17], and the total immersion liquid is 20 L. Because the ratio of H_2SO_4 to $CaSO_4 \cdot 2H_2O$ is 1:1, so we need a total mount of 2432 mL diluted sulfuric acid (0.125 mol/L) for the complete precipitation of $CaSO_4 \cdot 2H_2O$.

As can be seen from Fig. 1, at the end of the experiment, none of the dilute sulfuric acid added in each group reached 2432 mL, that is, the concentrations of $CaSO_4 \cdot 2H_2O$ produced in each group did not reach the theoretical value and were all dissolved in the immersion liquid. Therefore, it can be inferred that the composition of the product layer of the specimen tested does not contain $CaSO_4 \cdot 2H_2O$.

3.5 SEM and XRD Analysis

In order to obtain the phase and composition information of the eroded surface of the tested specimen, the composition of the coating was analyzed by SEM and XRD. Fig. 2 and Fig. 3 respectively show the microscopic topography of the corrosion surface and the phase spectrum of the corrosion layer in the first group and the sixth group.

As can be seen from Fig. 4a and Fig. 5a, no acicular or prismatic crystals were found on the eroded surfaces of the two batches of mortar specimens, suggesting no formation of gypsum ($CaSO4 \cdot 2H_2O$ and ettringite).

Further XRD analysis was performed on the phase composition of the eroded surface of the specimen. It can be seen from Fig. 4b and Fig. 5b that the XRD spectra of the corrosion layer of two batches of specimens were all SiO_2, and the diffraction peaks of $CaSO_4 \cdot 2H_2O$ and AFt were not found. This is due to the continuous dissolution of cement stone during the corrosion process, which lead to increased concentration of SiO_2. Since SiO_2 does not react with diluted sulfuric acid solution, more and more SiO_2 attaches to the surface of cement mortar specimens

and hinders the reaction. Therefore, in the absence of precipated $CaSO_4 \cdot 2H_2O$, the main component of the product layer is SiO_2.

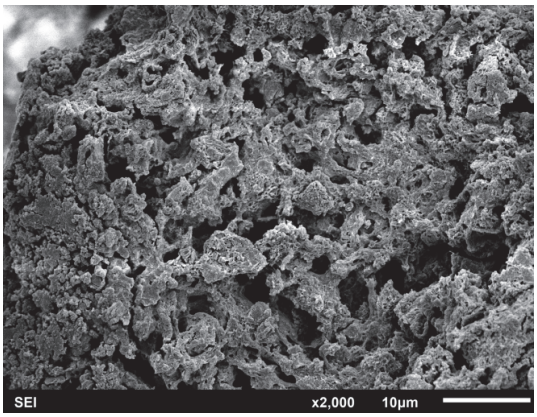

(a) Group 1

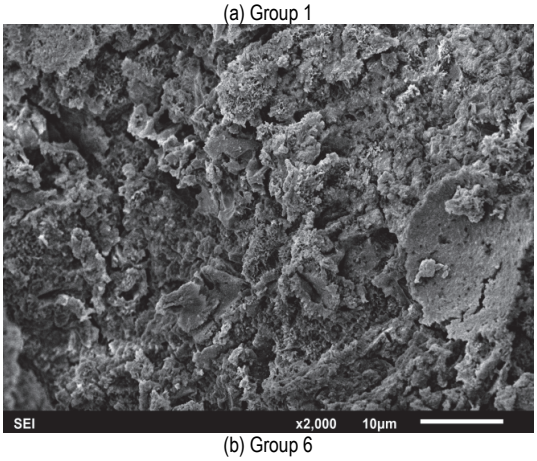

(b) Group 6

Figure 4 SEM photographs of group 1 and group 6

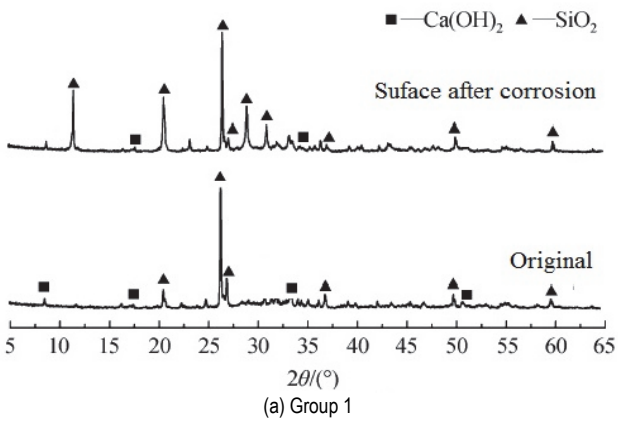

(a) Group 1

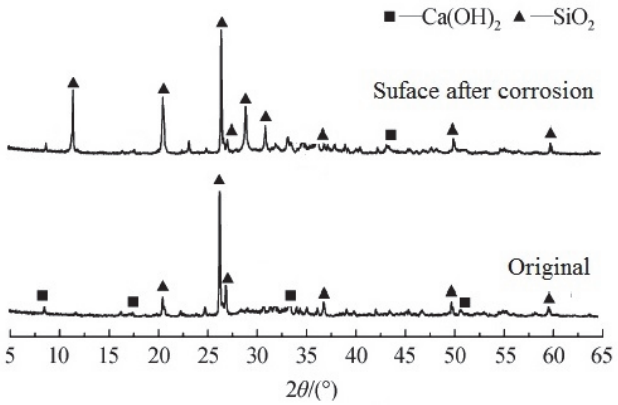

(b) Group 6

Figure 5 XRD patterns of original and vitriol corrosion group 1 and group 6

4 CONCLUSION

In this paper, the effect of the product layer produced by sulfuric acid corrosion of cement mortar and the specific composition of the product layer were studied. The results showed that:

(1) The corrosion rate reduces no matter the immersion liquid is changed or not, indicating the surface coating effect will occur under both immersion modes. By changing the soaking solution and removing the adhesion layer, the surface coating effect is reduced.

(2) Due to the product layer effect, when the reaction proceeds beyond the initial stage, the apparent diffusion coefficient decreases with immersion time in form of a power function of the latter.

(3) The precipitation analysis of the corrosion product shows that calcium sulfate does not precipitate within 2300h. The analysis of the corrosion surface by SEM and XRD indicates that the main component of the product layer is not calcium sulfate but silicon. Therefore, it can be inferred that the $CaSO_4 \cdot 2H_2O$ generated during the early stages of reaction is not enough to form an adhesion layer and the main component of the adhesion layer is SiO_2.

Acknowledgements

This work was supported by the Natural Science Foundation of China and Yunnan Province (Grant No. 51078175).

5 REFERENCES

[1] Du, Y. J., Wei, M. L., Reddy, K. R., Liu, Z. P., & Jin, F. (2014). Effect of acid rain pH on leaching behavior of cement stabilized lead-contaminated soil. *Journal of hazardous materials*, *14*(271), 131-140. https://doi.org/10.1016/j.jhazmat.2014.02.002

[2] Livingston, R. A. (2016). Acid rain attack on outdoor sculpture in perspective. *Atmospheric Environment*, *16*(146), 332-345. https://doi.org/10.1016/j.atmosenv.2016.08.029

[3] Rosso, F., Jin, W., Pisello, A. L., Ferrero, M., & Ghandehari M. (2016). Translucent marbles for building envelope applications: Weathering effects on surface lightness and finishing when exposed to simulated acid rain. *Construction and Building Materials*, *16*(108), 146-153. https://doi.org/10.1016/j.conbuildmat.2016.01.041

[4] Fan, Z. W. (2015). The effects of nano-calcined kaolinite clay on cement mortar exposed to acid deposits, *Construction and Building Materials*, *16*(102) , 486-495. https://doi.org/10.1016/j.conbuildmat.2015.11.016

[5] Chidiac, S. E. & Panesar, D. K. (2007). Evolution of mechanical properties of concrete containing ground granulated blast furnace slag and effects on the scaling resistance test at 28 days. *Cement and Concrete Composites*, *30*(2), 63-71. https://doi.org/10.1016/j.cemconcomp.2007.09.003

[6] Lee, H., Cody, R. D., & Cody, A. M. (2004). The formation and role of ettringite in Iowa highway concrete deterioration. *Cement and Concrete Research*, *35*(2), 332-343. https://doi.org/10.1016/j.cemconres.2004.05.029

[7] Pavlík, V., Bajza, A., & Rouseková, I. (2007). Degradation of concrete by flue gases from coal combustion. *Cement and concrete research*, *37*(7), 1085-1095. https://doi.org/10.1016/j.cemconres.2007.04.008

[8] Sun, X., Jiang, G., & Bond, P. L. (2014). A rapid, non-destructive methodology to monitor activity of sulfide-induced corrosion of concrete based on H_2S uptake rate.

Water Research, *14*(59), 229-238. https://doi.org/10.1016/j.watres.2014.04.016
[9] Connell, M., McNally, C., & Richardson, M. G. (2010). Biochemical attack on concrete in wastewater applications: A state of the art review. *Cement and Concrete Composites*, *32*(7), 479-485. https://doi.org/10.1016/j.cemconcomp.2010.05.001
[10] Yuan, H., Dangla, P., & Chatellier, P. (2015). Degradation modeling of concrete submitted to biogenic acid attack. *Cement and Concrete Research*, *15*(70), 29-38. https://doi.org/10.1016/j.cemconres.2015.01.002
[11] Jiang, G., & Sun, X., Keller, J. (2015). Identification of controlling factors for the initiation of corrosion of fresh concrete sewers. *Water research*, *25*(80), 30-40. https://doi.org/10.1016/j.watres.2015.04.015
[12] Pavlik, V. (2007). Degradation of Concrete by Flue Gases from Coal Combustion. *Cement and Concrete Research*, *37*(7), 1085-1095. https://doi.org/10.1016/j.cemconres.2007.04.008
[13] Israel, D., Macphee, D. E., & Lachowski, E. E. (1997). Acid attack on pore-reduced cements. *Journal of materials science*, *32*(15), 4109-4116. https://doi.org/10.1023/A:1018610109429
[14] Monteny, J., Belie, D., & Vincke, N.E. (2001). Chemical and microbiological tests to simulate sulfuric acid corrosion of polymer-modified concrete. *Cement and Concrete Research*, *31*(9), 1359-1365. https://doi.org/10.1016/S0008-8846(01)00565-8
[15] Gutberlet, T., Hilbig, H., & Beddoe, R. E. (2015). Acid attack on hydrated cement effect of mineral acids on the degradation process. *Cement and Concrete Research*, *15*(74), 35-43. https://doi.org/10.1016/j.cemconres.2015.03.011
[16] Xie, S. D., Zhou, D., & Yue, Q. X. (2016). Studies on the effect of simulated acid rain on the strength, phase and pore structure of mortar. *Acta Scientiae Circumstantiae*, *17* (1), 25-31.
[17] Min, H. G. (2010). Experimental research on the sulfate corrosion resistance of concrete and cement mortar. *Kunming University of Science and Technology*, *10*(1), 28-31.
[18] Feng, J. & Yan, P. Y. (2017). Performance and microstructure of oil well cement stone after sulfuric acid corrosion. *Chinese Journal of Silicomium*, *40*(05), 671-676.
[19] Zhigang, S. & Xue, S. (2010). Experimental study on corrosion of mortar by dilute sulfuric acid". *Chinese Journal of Building Materials*, *15*(02), 163-167.
[20] Liu, J., & Vipulanandan, C. (2018). Modeling water and sulfuric acid transport through coated cement concrete. *Journal of engineering mechanics*, *129*(4), 426-437. https://doi.org/10.1061/(ASCE)0733-9399(2003)129:4(426)
[21] Wells, T. & Melchers, R. E. (2015). Modelling concrete deterioration in sewers using theory and field observations. *Cement and Concrete Research*, *77*(12), 82-96. https://doi.org/10.1016/j.cemconres.2015.07.003
[22] Song, Z. G. (2013). Concentration Boundary Layer Model of Mortar Corrosion by Sulfuric Acid. *Journal of Wuhan University of Technology-Mater*, *26*(3), 527-532. https://doi.org/10.1007/s11595-011-0262-9
[23] Hewayde, H., Nehdi, M. E., & Allouche, E. (2006). Effect of geopolymer cement on microstructure, compressive strength and sulphuric acid resistance of concrete. *Magazine of Concrete Research*, *58*(5), 321-331. https://doi.org/10.1680/macr.2006.58.5.321
[24] Sun, X., Jiang, G., & Bond, P. L. (2019). A novel and simple treatment for control of sulfide induced sewer concrete corrosion using free nitrous acid. *Water research*, *70*(17), 279-287. https://doi.org/10.1016/j.watres.2014.12.020
[25] Etteyeb, N., Dhouibi, L., & Takenouti, H. (2014). Protection of reinforcement steel corrosion by phenyl phosphonic acid pre-treatment PART I: Tests in solutions simulating the electrolyte in the pores of fresh concrete. *Cement and Concrete Composites*, *55*(24), 241-249. https://doi.org/10.1016/j.cemconcomp.2014.07.025
[26] Ehrich, S., Helard, L., & Letourneux, R. (2019). Biogenic and chemical sulfuric acid corrosion of mortars. *Journal of materials in civil engineering*, *11*(4), 340-344. https://doi.org/10.1061/(ASCE)0899-1561(1999)11:4(340)

Contact information:

Weihang ZHANG
Faculty of Civil Engineering,
Kunming University of Science and Technology,
Kunming, China

Zhigang SONG
(Corresponding author)
Faculty of Civil Engineering,
Kunming University of Science and Technology,
Kunming, China
E-mail: songzhigang_kust@163.com